Systematic defect donor levels in III-V and II-VI semiconductors revealed by hybrid functional density-functional theory

Guido Petretto and Fabien Bruneval
CEA, DEN, Service de Recherches de Métallurgie Physique, F-91191 Gif-sur-Yvette, France
(Received 1 July 2015; revised manuscript received 2 December 2015; published 21 December 2015)

The identification of defect levels from photoluminescence spectroscopy is a useful but challenging task. Density-functional theory (DFT) is a highly valuable tool to this aim. However, the semilocal approximations of DFT that are affected by a band gap underestimation are not reliable to evaluate defect properties, such as charge transition levels. It is now established that hybrid functional approximations to DFT improve the defect description in semiconductors. Here we demonstrate that the use of hybrid functionals systematically stabilizes donor defect states in the lower part of the band gap for many defects, impurities or vacancies, in III-V and in II-VI semiconductors, even though these defects are usually considered as acceptors. These donor defect states are a very general feature and, to the best of our knowledge, have been overlooked in previous studies. The states we identify here may challenge the older assignments to photoluminescent peaks. Though appealing to screen quickly through the possible stable charge states of a defect, semilocal approximations should not be trusted for that purpose.

DOI: 10.1103/PhysRevB.92.224111 PACS number(s): 71.15.Mb, 61.72.J−, 61.72.uj, 78.55.−m

I. INTRODUCTION

Defects in a material have a role of paramount importance in determining its physical properties. Their presence has thus been extensively exploited to engineer devices with the desired features. When it comes to semiconductors, the introduction of electrically active defects causes an increase of the number of charge carriers in the conduction and valence bands, allowing one to tune the transport properties of the material. This is a key property for the preparation of most common electronic devices, like, e.g., transistors, LEDs, and solar cells [1].

In order to efficiently produce functional materials, it is mandatory to accurately identify which levels the defects introduce in the band gap and their position with respect to the band edges. To address this task, density functional theory (DFT) has been recognized as a highly valuable tool to interpret the experimental results and guide towards the choice of the most effective defect candidates to achieve doping. Despite its successes, DFT calculations rely on several approximations that can spoil the results and lead to qualitatively incorrect conclusions. For the positioning of the defect levels, the main source of error is the, sometimes severe, underestimation of the band gap that affects almost all the semilocal approximations to the exchange-correlation (xc) functional. In the latest years, hybrid functionals, defined by an admixture of exact and semilocal exchange, have improved the description of the band gap and thus of the defect transition energies [2], demanding an upgrade of the results previously calculated within the semilocal approximation

An edifying example is provided by the numerous defect candidates that have been considered as possible sources of p-type doping in ZnO, based on semilocal DFT calculations and that have been later recognized as deep acceptors, thanks to the improved results obtained from hybrid functional calculations [3–6].

Since the use of hybrid functionals leads to a considerable increase of the calculated band gaps, it is reasonable to expect an increase of the number of transition levels in the gap. Care should then be taken when studying these properties, since transitions to charge states that are missing in the semilocal approximation can emerge when using more accurate tools.

In this paper, we consider II-VI and III-V binary compounds, demonstrating the systematic emergence of positive charge states for defects that are usually considered as acceptors, like cation vacancies and anion substitutional defects. We relate this fact to the asymmetric downshift of the band edges and to the localization of holes introduced in the system. These additional charge states can change the perspective on this broad family of defects and on their actual suitability to achieve p-type doping.

II. COMPUTATIONAL DETAILS

All the simulations were performed using the VASP code within the projector augmented wave methodology [7–9]. The Perdew-Burke-Ernzerhof (PBE) [10] is used as a semilocal xc functional, while the hybrid functional is the one proposed by Heyd, Scuseria, and Ernzerhof (HSE) [11,12]. In the HSE approximation, a fraction α of the PBE exchange is replaced by exact exchange (EXX). In its original formulation $\alpha = 25\%$, but several schemes have been proposed to fix this value to obtain more accurate results [13,14]. In this work, we will consider α as a variable parameter, in order to explore its relationship with the position of the transition levels. A plane-wave cutoff energy of 400 eV has been used for ZnO, CdO, and GaN, 280 eV for ZnS, ZnSe, and ZnTe, and 212 eV for MgSe, while the Brillouin zone has been sampled at the Γ point in order to preserve electronic state degeneracies. We use 192-atom supercells for ZnO and GaN in the wurzite phase and 216-atom supercells for the other materials in the zinc-blende phase. The convergence with respect to the supercell size is demonstrated in the next paragraph.

For Zn and Ga, the $3d$ states are considered as valence electrons. The structures have been relaxed for each choice of the xc functional. The formation energies of the defects have been calculated according to the Zhang and Northrup formalism [15]. A monopole charge correction [6,16,17] has

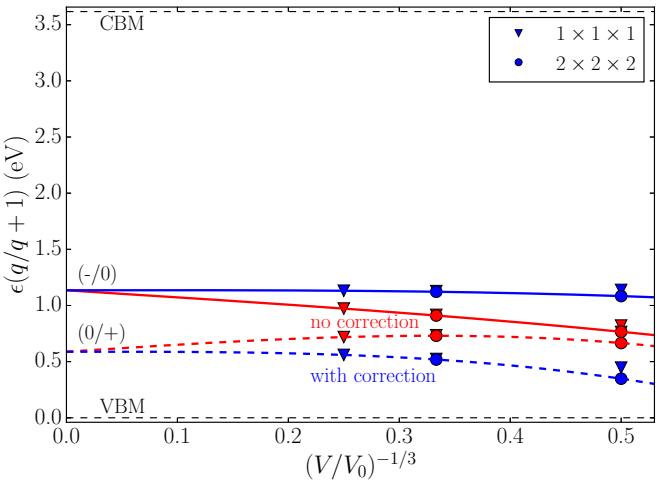

FIG. 1. (Color online) Dependence of the $(-/0)$ and $(0/+)$ transitions on the supercell size for the Mg vacancy in MgSe with (blue) and without (red) monopole charge correction. Values have been calculated with a Γ (triangle) and $2 \times 2 \times 2$ (circle) sampling of the Brillouin zone. Solid and dashed lines show a fit (see text) of the calculated values for the $(-/0)$ and $(0/+)$, respectively.

been added to speed up the convergence, where the dielectric tensors have been taken from experimental measurements.

In order to verify the accurateness of our approximations, we have studied the convergence of the $(-/0)$ and the shallower $(0/+)$ transitions for the Mg vacancy in MgSe as a function of the supercell size and sampling of the Brillouin zone. As the defect wave function might change according to the exchange-correlation type, we performed a convergence study for the very functional we are to employ in this study, namely, HSE. We considered up to 512 atoms and a $2 \times 2 \times 2$ k-point sampling. As shown in Fig. 1, once the charge correction is taken into account, the calculated value for the 216-atom supercell gives a value of the transition energy that is in agreement with the value extrapolated from the fit $aV^{-1/3} + bV^{-1} + c$ in the limit $V \to \infty$, where V is the volume of the supercell. The error is less than 65 meV for the $(0/+)$ transition level and less than 8 meV for the $(-/0)$ one. Note that the finite-size correction works extremely well for the deep transitions, whereas its efficiency is more limited for the states closer to the band edges. Anyway, as the charge corrections increase the energy of the charged supercells, applying the charge corrections systematically cannot spuriously stabilize the $(0/+)$ donor transition levels this study is focused on. We can conclude that these additional states are not an artifact of a too small supercell size. In addition, for the 216-atom supercell size that we have chosen, the differences between the transition energies for the Γ and $2 \times 2 \times 2$ sampling are smaller than 6 meV. The k-point sampling is clearly not an issue here.

III. EMERGENCE OF DONOR LEVELS

The effect of introducing a portion of EXX in the xc functional has a strong effect on the band gap. With $\alpha = 25\%$ all the gaps studied here are increased by at least 1 eV with respect to the PBE value, with the largest increase in the case of ZnO and GaN, where the band gaps go from 0.69 to 2.48 eV and

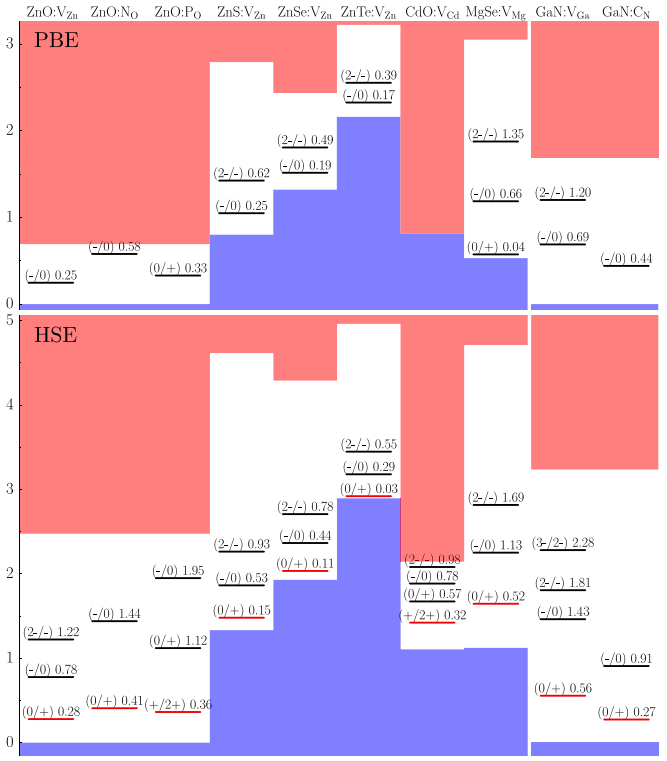

FIG. 2. (Color online) Transition energies for (q/q') transitions with PBE (top) and HSE (bottom) approximations. The VBMs of II-VI compounds are aligned according to Ref. [21] with corrections to take into account functional and volume changes. The GaN is not aligned with respect to the other materials. Positive charge states entering the band gap in HSE are highlighted in red.

from 1.69 to 3.25 eV, respectively. Despite these considerable increases, it has been shown that, for localized defects, once it is referred to an external reference (e.g., the average of the electrostatic potential), the transition level should have a small dependence with respect to the approximation employed [18,19]. This conclusion can be slightly altered by geometric relaxation, that can give rise to rather different structures in the surrounding of the defect depending on the xc functional [5], but this effect is often negligible [20].

In this picture, it is possible for transition levels lying beyond the band edges in the semilocal approximations to end up in the band gap as a consequence of the band edges shift. In Fig. 2, we report a series of materials with defects in which such an effect actually takes place: the cation vacancies and some remarkable substitutional defects, namely, N_O and P_O in ZnO and C_N in GaN. The valence band maxima (VBM) are aligned according to the data reported by Li *et al.* [21], with additional shifts to take into account the different functionals employed and the differences in the supercell volume, quantified through the deformation potentials, when available in literature [22–24].[1]

[1]No deformation potential is available for MgSe. Since this is generally small, we neglected that correction in this case. The deformation potential shows little dependence on the phase [22] and thus we used the zinc-blende values in the case of ZnO and GaN.

Figure 2 strikingly shows that, although the defects would be considered in a simple ionic model as single (substitutional defect), double (cation vacancies in II-VI), and triple (V_{Ga} in GaN) acceptors, all of them exhibit stable positive charge states within HSE, with a (0/+) transition inside the band gap and, in some cases, even a (+/2+) transition. With few exceptions, these transitions are all at least 0.3 eV away from the VBM, with a maximum of 1.12 eV in the case of the P_O. It is worth noting that in this last case, as well as for the V_{Mg} defect in MgSe, a (0/+) transition is present even at the PBE level, signaling that the stabilization of the positive charge states is not uniquely related to the introduction of the EXX.

Comparing the cation vacancies in the II-VI compounds, the transition energies of zinc chalcogenides (ZnO, ZnS, ZnSe, ZnTe) become shallower with increasing VBM. However, this statement does not hold when turning to CdO and MgSe. We thus conclude that a low absolute value of the VBM can favor the presence of additional charge states in the lower part of the band gap with deeper transition energies, although the presence of such states cannot be excluded by solely monitoring the position of the VBM.

The defects shown in Fig. 2 share a common feature: they all present holes that are strongly localized in the vicinity of the defect. This localization can be expected to be favored by the inclusion of EXX. In fact, it has been demonstrated [25] that, when going beyond standard DFT approximations, the zinc vacancy in zinc chalcogenides presents holes localized on the chalcogen nearest neighbor, with an increase of the distance of these atoms from the vacancy [25]. So, while in the semilocal approximation the local symmetry of the defect is always a tetrahedral one (T_d), within HSE, the local symmetry is lowered from T_d to C_{3v} and to C_{2v} when going from 2− up to the neutral charge state. Given that the holes are localized far apart from each other, this leaves room for the addition of two further holes to reach a 2+ charge state. In Fig. 3, the spin densities for V_{Zn} in ZnO for charge states from 1− to 2+ are shown as a prototypical example. The additional holes are localized on the remaining O neighbors with a subsequent lowering of the symmetry to C_{3v} in the 1+ charge state and the restoration of the T_d symmetry when reaching the 2+ charge state. This pattern is clearly identified for ZnO, CdO, and MgSe, while for the other zinc chalcogenides the spin density is more delocalized in the positive charge states. This discrepancy is due to the shallower nature of the (0/+) transitions in ZnS, ZnSe, and ZnTe. GaN represents a different case since V_{Ga} is a triple acceptor and one could expect three localized holes in the neutral state. However, at $\alpha = 0.25$, the spin density tends to be more delocalized on the four neighbors and a larger value of α is required to localize it on the expected number of neighbors. We stress that the energy difference between low and high spin configurations is remarkably small, with only a slight preference for high spin configurations in several cases. Even in the case of low spin configuration resulting in a vanishing net spin, it is crucial to carry out spin-unrestricted calculations that allow for a much lower total energy compared to spin-restricted calculations.

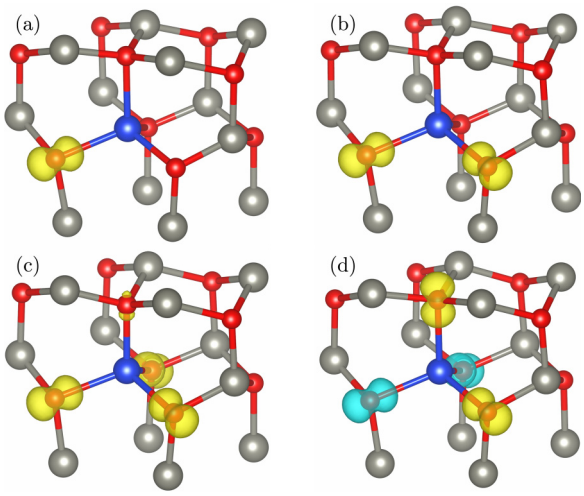

FIG. 3. (Color online) Spin-up (yellow) and spin-down (light blue) densities for V_{Zn} in ZnO in the (a) 1−, (b) 0, (c) 1+, and (d) 2+ charge states. Zn and O atoms are shown as grey and red spheres, respectively, while the blue sphere represents the original position of the missing Zn atom. The holes are localized on the vacancy nearest neighbors.

In the substitutional defects, at variance with the PBE approximation, HSE calculations show holes localized on the impurities along one of the bonds [5] and offer the possibility of localizing additional holes along other bonds. Due to the different localization of holes in HSE in ZnO and GaN, the transition levels in HSE deviate from the simple shift of the VBM obtained within PBE.

Positive charge states for some substitutional defects in zinc calchogenides have already been predicted, but their presence has been related to the formation of specific AX centers [26]. We argue here that the positive charge states are instead a systematic feature. As an additional confirmation of this picture, none of the defects show additional negative charge states in the upper part of the band gap, apart from those consistent with the nature of single, double and triple acceptor of the defects discussed. In fact, once the acceptor is completely passivated, there is no further room to accommodate additional electrons.

IV. DEPENDENCE ON THE EXACT EXCHANGE FRACTION

Since the positive charge states are also present when the holes are more delocalized, a relevant contribution for their emergence is given by the shift of the band edges. As shown by Chen and Pasquarello [27,28], the downshift of the VBM plays a dominant role in the opening of the band gap for most semiconductors and this enhances the possibility for defects states which are spuriously below the VBM in PBE to enter inside the band gap in higher-level approximations. So far, we had set the α parameter to its original value of 25%. However, this parameter is often increased to better fit experimental band gaps and thus leading to even larger shifts of the band edges. In order to evaluate the sensitivity upon this parameter of the position of the new states that we identify, it is instructive to analyze the transition energies as a function of α.

We first focus on the case of ZnO, where a large value $\alpha = 0.375$ is indeed required to match the experimental band gap [29]. Figure 4 shows the comparison between

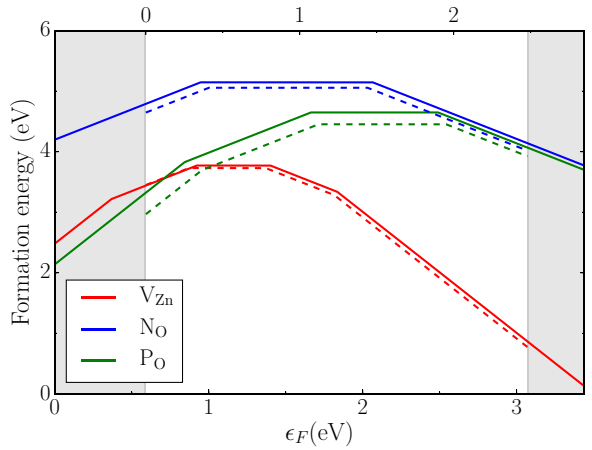

FIG. 4. (Color online) Formation energy as a function of the Fermi level ϵ_F for defects in ZnO in HSE approximation with $\alpha = 0.25$ (top axis, dashed lines) and $\alpha = 0.375$ (bottom axis, solid lines). The formation energies across the different values of α have been aligned with respect to the average electrostatic potential. Shaded areas represent the shifts of the band edges.

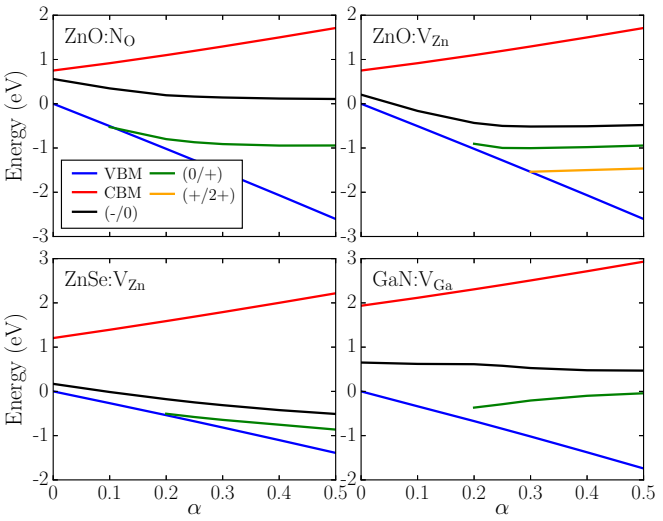

FIG. 5. (Color online) Dependence of the VBM, CBM and $E_{\text{diff}}(q/q+1)$ of Eq. (1) from the α of HSE for defects in ZnO, ZnSe, and GaN. The energy differences E_{diff} are shown only for values of α such that $E_{\text{diff}} > \epsilon_{\text{VBM}}$.

the formation energies of the various defects in ZnO, as a function of the Fermi level ϵ_F, for $\alpha = 0.25$ and 0.375. For all these defects, the formation energies and the position of the transition energies have little dependence on α, once they have been referred to average electrostatic potential.[2] In this range, the holes are always well localized and the small changes observed are mainly due to different structural relaxation. As a consequence, the change in the depth of the transition energies is almost completely related to the downshift of the VBM that amounts to 0.6 eV. This may lead to even more defect levels inside the gap, as is the case for V_{Zn}: the 2+ charge state is stabilized, with a (+/2+) transition energy of 0.36 eV.

To figure out a general picture of the emergence of defect levels across defects and materials, we have analyzed the α dependence of the transition energies starting from $\alpha = 0$, that is equivalent to the simple PBE approximation, to a large value of 0.5. The transition energies under study can be defined as

$$\begin{aligned}\epsilon(q/q+1) &= E_{\text{tot}}[D^q] - E_{\text{tot}}[D^{q+1}] + \epsilon_{\text{c}} - \epsilon_{\text{VBM}} \\ &= E_{\text{diff}}(q/q+1) - \epsilon_{\text{VBM}}, \end{aligned} \quad (1)$$

where $E_{\text{tot}}[D^q]$ is the DFT energy for the defect D in charge state q, ϵ_{VBM} is the VBM energy and ϵ_{c} represents the corrections due to the finite size of the supercell. $\epsilon(q/q+1)$ can be then decomposed into two contributions ϵ_{VBM} and the remainder $E_{\text{diff}}(q/q+1)$. For the transition to be inside the band gap, the condition $E_{\text{diff}}(q/q+1) > \epsilon_{\text{VBM}}$ should be satisfied. Figure 5 contains the value of the band edges and total energy differences $E_{\text{diff}}(q/q+1)$ for some of the defects considered, showing different trends in the emergence of positive charge states as α increases. The partition of the transition energy into these two components allows us to distinguish the contribution of the downshift of the VBM from the one due to the change in the defect energy.

For all the semiconductors that we have considered here the dependence of the absolute positioning of the VBM on the EXX content is massive. When changing α from zero to 25%, the downshift ranges from 0.8 to 1.5 eV. This general phenomenon is clearly the most significant cause for the presence of additional charge states in the band gap. Note that the large dependence of the VBM upon the xc is confirmed by higher level calculations in the GW approximation [27,28].

The term $E_{\text{diff}}(q/q+1)$ is completely analogous to the ΔSCF evaluation of the ionization energy used for finite systems, in which a total energy difference between the neutral and the charged systems brings a rather stable evaluation of the ionization energy when changing the xc approximation. On the contrary, the evaluation with the eigenvalues, the so-called Koopmans' theorem, is much more delicate. Then the total energy difference $E_{\text{diff}}(q/q+1)$ presents three different behaviors in Fig. 5 according to the nature of the states.

First case. The state under scrutiny follows one of the band edges when α varies. This indicates that the corresponding electronic wave function is of the same nature of the band edge and that is quite delocalized around the defect. This is the case we observe for the low values of α in ZnO for N_O as well as for V_{Zn}. For these two defects, even the $(-/0)$ transition that is deep inside the band gap shows this trend. In ZnSe, the $(-/0)$ transition also shows this behavior, but for the whole range of α, as does the $(0/+)$ transition after entering the gap.

Second case. The state is independent from the value of α. This behavior indicates a localized electronic state for which the ΔSCF procedure is producing a stable evaluation for the ionization energy. This is the situation we observe for N_O and V_{Zn} in ZnO when α is larger than 0.25% and for the $(-/0)$ transition in GaN.

Third case. The state behaves in a way that cannot be rationalized by the first two cases. This is what we observe

[2]When aligning two systems with different values of α, inaccuracies can emerge from the ill-defined electrostatic potential, which is known up to a constant. As demonstrated in Ref. [28], these errors are any way small and this contribution was neglected here.

for the $(0/+)$ transition in V_{Ga} in GaN. This complex behavior results from a combination of effects, such as a change in the nature of the state along with α, a localization of the hole, and a change of the atomic relaxation.

Figure 5 shows how localized states are inserted in the band gap: either these states were not localized with low values of α and become localized with larger α or the states were already localized for $\alpha = 0$ but were positioned below the VBM. In every case, the additional states emerge at relatively low values of α, so their presence should always be considered, no matter the scheme used to fix the amount of EXX.

V. CONCLUSIONS

To summarize, we have shown the existence of positive charge states for defects usually considered as pure acceptors in II-VI and III-V compounds that become stable when moving from a semilocal to a hybrid approximation of the xc functional. We have related this to two factors: the increase of the holes localization, induced by the portion of EXX in hybrid functional, and the strong downshift of the VBM.

The presence of these transition levels inside the band gap can have important consequences in the analysis and design of defective materials. Since to achieve p-type doping shallow acceptors are needed, several among the defects considered here have been investigated as possible sources of holes. However, if close to the VBM the most stable states are positively charged, these defects can act as compensating defects instead. From a theoretical point of view, it is then important to always check for further stable charge states, when moving from semilocal to higher level approximations of the xc functional.

Even though we limited our analysis to acceptor defects, it is likely that similar effects could be observed for donor defects as well. Based on our results, we speculate that the appearance of negative charge states for donors could be favored by defects with highly localized electrons and materials displaying a non-negligible upshift of the conduction band minimum.

ACKNOWLEDGMENTS

This work was supported by the French "Agence Nationale de la Recherche" (Project No. ANR-11-NANO-013). This work was performed using HPC resources from GENCI-IDRIS and GENCI-TGCC (Grant 2014-gen6018).

[1] S. M. Sze and K. K. Ng, *Physics of Semiconductor Devices* (Wiley, New York, 2006).

[2] Christoph Freysoldt, Blazej Grabowski, Tilmann Hickel, Jörg Neugebauer, Georg Kresse, Anderson Janotti, and Chris G. Van de Walle, First-principles calculations for point defects in solids, Rev. Mod. Phys. **86**, 253 (2014).

[3] J. L. Lyons, A. Janotti, and C. G. Van de Walle, Why nitrogen cannot lead to p-type conductivity in zno, Appl. Phys. Lett. **95**, 252105 (2009).

[4] B. Puchala and D. Morgan, Stable interstitial dopant–vacancy complexes in zno, Phys. Rev. B **85**, 195207 (2012).

[5] Stephan Lany and Alex Zunger, Generalized koopmans density functional calculations reveal the deep acceptor state of n_o in zno, Phys. Rev. B **81**, 205209 (2010).

[6] Guido Petretto and Fabien Bruneval, Comprehensive ab initio study of doping in bulk zno with group-v elements, Phys. Rev. Appl. **1**, 024005 (2014).

[7] G. Kresse and J. Furthmüller, Efficient iterative schemes for *ab initio* total-energy calculations using a plane-wave basis set, Phys. Rev. B **54**, 11169 (1996).

[8] G. Kresse and D. Joubert, From ultrasoft pseudopotentials to the projector augmented-wave method, Phys. Rev. B **59**, 1758 (1999).

[9] P. E. Blöchl, Projector augmented-wave method, Phys. Rev. B **50**, 17953 (1994).

[10] John P. Perdew, Kieron Burke, and Matthias Ernzerhof, Generalized Gradient Approximation Made Simple, Phys. Rev. Lett. **77**, 3865 (1996).

[11] J. Heyd, G. E. Scuseria, and M. Ernzerhof, Hybrid functionals based on a screened coulomb potential, J. Chem. Phys. **118**, 8207 (2003).

[12] J. Heyd, G. E. Scuseria, and M. Ernzerhof, Erratum: hybrid functionals based on a screened coulomb potential [J. Chem. Phys. **118**, 8207 (2003)], J. Chem. Phys. **124**, 219906 (2006).

[13] Miguel A. L. Marques, Julien Vidal, Micael J. T. Oliveira, Lucia Reining, and Silvana Botti, Density-based mixing parameter for hybrid functionals, Phys. Rev. B **83**, 035119 (2011).

[14] R. Ramprasad, H. Zhu, Patrick Rinke, and Matthias Scheffler, New Perspective on Formation Energies and Energy Levels of Point Defects in Nonmetals, Phys. Rev. Lett. **108**, 066404 (2012).

[15] S. B. Zhang and John E. Northrup, Chemical Potential Dependence of Defect Formation Energies in Gaas: Application to Ga Self-Diffusion, Phys. Rev. Lett. **67**, 2339 (1991).

[16] M. Leslie and N. J. Gillan, The energy and elastic dipole tensor of defects in ionic crystals calculated by the supercell method, J. Phys. C **18**, 973 (1985).

[17] R. Rurali and X. Cartoixà, Theory of defects in one-dimensional systems: Application to Al-catalyzed Si nanowires, Nano Lett. **9**, 975 (2009).

[18] Audrius Alkauskas, Peter Broqvist, and Alfredo Pasquarello, Defect Energy Levels in Density Functional Calculations: Alignment and Band Gap Problem, Phys. Rev. Lett. **101**, 046405 (2008).

[19] Wei Chen and Alfredo Pasquarello, Correspondence of defect energy levels in hybrid density functional theory and many-body perturbation theory, Phys. Rev. B **88**, 115104 (2013).

[20] Audrius Alkauskas and Alfredo Pasquarello, Band-edge problem in the theoretical determination of defect energy levels: The o vacancy in zno as a benchmark case, Phys. Rev. B **84**, 125206 (2011).

[21] Yong-Hua Li, Aron Walsh, Shiyou Chen, Wan-Jian Yin, Ji-Hui Yang, Jingbo Li, Juarez L. F. Da Silva, X. G. Gong, and Su-Huai

Wei, Revised *ab initio* natural band offsets of all group iv, ii-vi, and iii-v semiconductors, Appl. Phys. Lett. **94**, 212109 (2009).

[22] Su-Huai Wei and Alex Zunger, Predicted band-gap pressure coefficients of all diamond and zinc-blende semiconductors: Chemical trends, Phys. Rev. B **60**, 5404 (1999).

[23] Yong-Hua Li, X. G. Gong, and Su-Huai Wei, *Ab initio* all-electron calculation of absolute volume deformation potentials of iv-iv, iii-v, and ii-vi semiconductors: The chemical trends, Phys. Rev. B **73**, 245206 (2006).

[24] Y. Z. Zhu, G. D. Chen, Honggang Ye, Aron Walsh, C. Y. Moon, and Su-Huai Wei, Electronic structure and phase stability of mgo, zno, cdo, and related ternary alloys, Phys. Rev. B **77**, 245209 (2008).

[25] J. A. Chan, Stephan Lany, and Alex Zunger, Electronic Correlation in Anion P Orbitals Impedes Ferromagnetism due to Cation Vacancies in zn Chalcogenides, Phys. Rev. Lett. **103**, 016404 (2009).

[26] Koushik Biswas and Mao-Hua Du, Ax centers in ii-vi semiconductors: Hybrid functional calculations, Appl. Phys. Lett. **98**, 181913 (2011).

[27] Wei Chen and Alfredo Pasquarello, Band-edge levels in semiconductors and insulators: Hybrid density functional theory versus many-body perturbation theory, Phys. Rev. B **86**, 035134 (2012).

[28] Wei Chen and Alfredo Pasquarello, Band-edge positions in gw: Effects of starting point and self-consistency, Phys. Rev. B **90**, 165133 (2014).

[29] Fumiyasu Oba, Atsushi Togo, Isao Tanaka, Joachim Paier, and Georg Kresse, Defect energetics in zno: A hybrid hartree-fock density functional study, Phys. Rev. B **77**, 245202 (2008).